Observational information for f(T) theories and Dark Torsion

Gabriel R. Bengochea[1,*]

[1] *Instituto de Astronomía y Física del Espacio (IAFE), CC 67, Suc. 28, 1428 Buenos Aires, Argentina*

In the present work we analyze and compare the information coming from different observational data sets in the context of a sort of f(T) theories. We perform a joint analysis with measurements of the most recent type Ia supernovae (SNe Ia), Baryon Acoustic Oscillation (BAO), Cosmic Microwave Background radiation (CMB), Gamma-Ray Bursts data (GRBs) and Hubble parameter observations (OHD) to constraint the only new parameter these theories have. It is shown that when the new combined BAO/CMB parameter is used to put constraints, the result is different from previous works. We also show that when we include Observational Hubble Data (OHD) the simpler LambdaCDM model is excluded to one sigma level, leading the effective equation of state of these theories to be of phantom type. Also, analyzing a tension criterion for SNe Ia and other observational sets, we obtain more consistent and better suited data sets to work with these theories.

I. INTRODUCTION

Current cosmological observations, mainly from type Ia supernovae, show that the universe is undergoing accelerated expansion [1–4]. This accelerated expansion has been attributed to a dark energy component with negative pressure. The simplest explanation for this dark energy seems to be the cosmological constant. However, among many candidates [5–7], some modified gravity models have also been proposed based on, for example, $f(R)$ theories [8–19].

Some models based on modified teleparallel gravity were presented as an alternative to inflationary models [20, 21] or showing a cosmological solution for the acceleration of the universe by means of a sort of theories of modified gravity, namely $f(L_T)$ [22], based on a modification of the Teleparallel Equivalent of General Relativity (TEGR) Lagrangian [23, 24] where *dark torsion* is the responsible for the observed acceleration of the universe, and the field equations are always 2nd order equations. It was shown in [22] that this fact makes these theories simpler than the dynamical equations resulting in $f(R)$ theories among other advantages. Recently, in [25] this sort of modified gravity theories was called $f(T)$ theories and some works have begun to develop in this area [26–35].

In [36] the tension and systematics in the Gold06 SNe Ia data set have been investigated in great detail. Other authors, working with different SNe Ia sets found these were in tension with other SNe Ia sets and also with BAO and CMB [37, 38]. In [37], analyzing the Union data set [2], the UnionT truncated data set was built by discarding the supernovae generating the tension by using the ΛCDM model to select the outliers. In [38], performing the same truncation procedure of [37] for 10 different models, it was suggested that the impact of different models would be negligible.

*Electronic address: gabriel@iafe.uba.ar

In this work we present thorough observational information useful to work with $f(T)$ theories by using the latest Union2 SNe Ia compilation released [3], the new combined parameter from Baryon Acoustic Oscillation and Cosmic Microwave Background radiation (BAO/CMB) [39] (more suitable for non-standard models than the usually used R and A parameters), a Gamma-Ray Burst data set [40] and constraints from Observational Hubble Data (OHD) [41–43].

This Letter is organized as follows: in Section II we review the fundamental concepts about $f(T)$ theories to, in Section III, analyze a criterion of tension to improve the study of the new data sets including BAO/CMB and GRBs. In Section IV we perform the truncation of Union2 calculating the relative deviation to the best fit of the $f(T)$ prediction for each one of the 557 points following [37, 38] in order to show the disappearing of tension and establishing a new set suitable for $f(T)$ theories. In Section V we add the OHD observational information and discuss some remarkable results and, in Section VI, we summarize the conclusions of this work.

II. GENERAL CONSIDERATIONS ABOUT $f(T)$ THEORIES

Teleparallelism [23, 24] uses as dynamical object a vierbein field $\mathbf{e}_i(x^\mu)$, $i = 0, 1, 2, 3$, which is an orthonormal basis for the tangent space at each point x^μ of the manifold: $\mathbf{e}_i \cdot \mathbf{e}_j = \eta_{i\,j}$, where $\eta_{i\,j} = diag(1, -1, -1, -1)$. Each vector $\mathbf{e}_i$ can be described by its components e_i^μ, $\mu = 0, 1, 2, 3$ in a coordinate basis; i.e. $\mathbf{e}_i = e_i^\mu \partial_\mu$. Notice that Latin indices refer to the tangent space, while Greek indices label coordinates on the manifold. The metric tensor is obtained from the dual vierbein as $g_{\mu\nu}(x) = \eta_{i\,j}\, e^i_\mu(x)\, e^j_\nu(x)$. Differing from General Relativity (GR), which uses the torsionless Levi-Cività connection, Teleparallelism uses the curvatureless Weitzenböck connection [44], whose non-null torsion is

$$T^\lambda_{\mu\nu} = \hat{\Gamma}^\lambda_{\nu\mu} - \hat{\Gamma}^\lambda_{\mu\nu} = e^\lambda_i \left(\partial_\mu e^i_\nu - \partial_\nu e^i_\mu\right) \qquad (1)$$

The TEGR Lagrangian is built with the torsion (1), and its dynamical equations for the vierbein imply the Einstein equations for the metric. The teleparallel Lagrangian is [24, 45, 46],

$$L_T \equiv T = S_\rho{}^{\mu\nu}\, T^\rho{}_{\mu\nu} \tag{2}$$

where:

$$S_\rho{}^{\mu\nu} = \frac{1}{2}\Big(K^{\mu\nu}{}_\rho + \delta^\mu_\rho\, T^{\theta\nu}{}_\theta - \delta^\nu_\rho\, T^{\theta\mu}{}_\theta\Big) \tag{3}$$

and $K^{\mu\nu}{}_\rho$ is the contorsion tensor:

$$K^{\mu\nu}{}_\rho = -\frac{1}{2}\Big(T^{\mu\nu}{}_\rho - T^{\nu\mu}{}_\rho - T_\rho{}^{\mu\nu}\Big) \tag{4}$$

which equals the difference between Weitzenböck and Levi-Cività connections.

For a flat homogeneous and isotropic Friedmann-Robertson-Walker universe (FRW),

$$e^i_\mu = diag(1, a(t), a(t), a(t)) \tag{5}$$

where $a(t)$ is the cosmological scale factor. By replacing in (1), (3) and (4) one obtains

$$T = S^{\rho\mu\nu} T_{\rho\mu\nu} = -6\,\frac{\dot{a}^2}{a^2} = -6\,H^2 \tag{6}$$

H being the Hubble parameter $H = \dot{a}\, a^{-1}$.

In these modified gravity theories, the action is built promoting T to a function $f(T)$. The case $f(T) = T$ corresponds to TEGR. In an $f(T)$ theory the spinless matter couples to the metric in the standard form. Therefore, the equations of a freely falling particle are the equations of the geodesics. Moreover, the source in the equations for the geometry results to be the matter energy-momentum tensor. In these aspects there is no difference with GR. If matter is distributed isotropically and homogeneously, the metric is the FRW metric and all kinematic equations (luminosity distance, angular distance, cosmological redshift, etc.) will be identical to the GR case. Any modification in the null geodesics followed by light rays will be exclusively in the scale factor $a(t)$. Some authors have mentioned that $f(T)$ theories are not invariant under local Lorentz transformations [20, 34]. However, if this would affect the viability of these models is a subject which is currently being analyzed.

The variation of the action with respect to the vierbein leads to the field equations,

$$e^{-1}\partial_\mu(e\, S_i{}^{\mu\nu}) f'(T) - e_i^\lambda\, T^\rho{}_{\mu\lambda}\, S_\rho{}^{\nu\mu} f'(T) + S_i{}^{\mu\nu}\partial_\mu(T) f''(T) + \frac{1}{4}\, e_i^\nu\, f(T) = 4\,\pi\, G\, e_i{}^\rho\, T_\rho{}^\nu \tag{7}$$

where a prime denotes differentiation with respect to T, $S_i{}^{\mu\nu} = e_i{}^\rho S_\rho{}^{\mu\nu}$ and $T_{\mu\nu}$ is the matter energy-momentum tensor.

The substitution of the vierbein (5) in (7) for $i = 0 = \nu$ yields

$$12\, H^2\, f'(T) + f(T) = 16\pi G\, \rho \tag{8}$$

Besides, the equation $i = 1 = \nu$ is

$$48 H^2 f''(T)\dot{H} - f'(T)[12H^2 + 4\dot{H}] - f(T) = 16\pi G\, p \tag{9}$$

In Eqs. (8-9), $\rho(t)$ and $p(t)$ are the total density and pressure respectively.

In [22] it was shown that when $f(T)$ is a power law such as

$$f(T) = T - \frac{\alpha}{(-T)^n} \tag{10}$$

leads to reproduce the observed accelerated expansion of the universe, being α and n real constants to be determined by observational constraints.

From (8) along with (10), the modified Friedmann equation results to be (e.g. [22])

$$H^2 - \frac{(2n+1)\,\alpha}{6^{n+1} H^{2n}} = \frac{8}{3}\pi G\rho \tag{11}$$

where $\rho = \rho_{mo}(1+z)^3 + \rho_{ro}(1+z)^4$, z is the cosmological redshift and as it is usual, we will call $\Omega_i = 8\pi G\,\rho_{io}/(3H_0^2)$ to the contributions of matter and radiation to the total energy density today. For $\alpha = 0$ the GR spatially flat Friedmann equation is retrieved. The case $n = 0$ recovers the GR dynamics with cosmological constant. Compared with GR, n is the sole new free parameter (see [22] for details).

In the next sections, we will use a $\chi^2 = \chi^2_{SNe} + \chi^2_{BAO/CMB} + \chi^2_{GRB} + \chi^2_{OHD}$ statistic to find best fits for the free parameters Ω_m and n of a model given by (10) using several data sets. The separate χ^2 of SNe Ia, BAO/CMB, GRBs and OHD and the corresponding data sets used in this work are shown in Appendix B. In order to see whether our model is favored over the ΛCDM model, we will also use the information criterion known as AIC (Akaike Information Criterion) [47, 48]. The AIC is defined as $AIC = -2 ln\mathcal{L}_{max} + 2k$, where the likelihood is defined as $\mathcal{L} \propto e^{\chi^2/2}$, the term $-2\, ln\mathcal{L}_{max}$ corresponds to the χ^2_{min} and k is the number of parameters of the model. According to this criterion a model with the smaller AIC is considered to be the best, and a difference $|\Delta AIC|$ in the range between 0 and 2 means that the two models have about the same support from the data. For a difference between 2 and 4 this support is considerably less for the model with the larger AIC, while for a difference >10 the model with the larger AIC is practically irrelevant [49].

III. CONSTRAINING DARK TORSION WITH UPDATED DATA SETS

We found interesting to analyze what would happen if we applied a criterion in order to study the consistency between data sets, a criterion more restrictive than the only fact that the confidence intervals overlap. To perform this analysis, we adopted the criterion of considering the existence of tension between a given data set and

another set constituted combining several data sets (including the first one) as the fact that the best fit point to the first data set is out of the 68.3% (1σ) confidence level contour given by the combined data set. Similar criteria were adopted in their analysis by [36–38]. One could choose not to use this more restrictive criterion; however, we wanted to investigate its consequences of applying it to several data sets in the framework of $f(T)$ theories. In [36], for example, the best fits to sets and subsets of SNe are compared with the means of determining if two of those are in tension or not, and how far from the confidence intervals lies the ΛCDM model. With our adopted criterion, we seek more physical consistency between best-fits, so the best fits do not drive to too different cosmological evolutions. The best fit which effective equation of state is of the phantom type [50] ($w_{eff} < -1$) tells us about very different physics from the one that is not. Also, best fits that lie too far apart from ΛCDM model ($n = 0$ or w_{eff}=-1) will indicate the need of more exotic models.

Something important to consider is that the best fits to the SNe or their combination depend also on the fitter used to process the SNe data sets. Avoiding this type of tension we make sure that in most cases both best fits (SNe Ia and combined data sets) have similar results in the equation of state w_{eff} or the n parameter. In the wCDM (w=const) framework, for example, it has been shown that with the SDSSII (MLCS) data set [51, 52] both best fits suggest different cosmic evolutions while when relieving the tension this problem disappears [53].

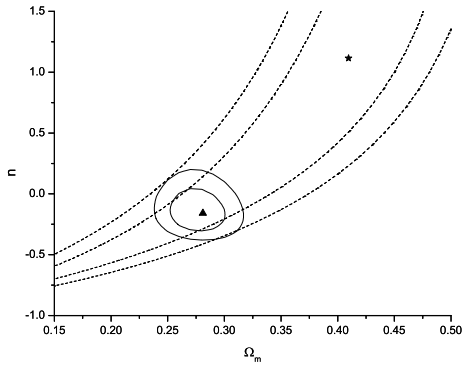

FIG. 1: Confidence intervals at 68.3% and 95.4% in the $\Omega_m - n$ plane for the UnionT observations of SNe Ia only (dashed lines) and UnionT SNe Ia, BAO and CMB (solid lines). We also show the best fit values to the observations of UnionT SNe Ia only (star), and to the combination of UnionT SNe Ia, BAO and CMB (triangle).

Then, with this criterion, in our previous work [22] existed some tension between the data from the SNe Ia Union sample [2] and BAO [54] and CMB [55]. Taking the truncated UnionT data set from [37] we proceeded to evaluate the possible tension between UnionT, BAO and CMB.

We found there was still tension between these data sets as shown in Fig. 1. On one hand, the best fit to SNe Ia is of the phantom type and the one corresponding to the combined set is not and, on the other hand, the best fit to SNe Ia drives H in recombination to be 20% greater than for the best fit to SNe+BAO+CMB, and w_{eff} today to be 35% greater. Considering the mentioned criterion, UnionT eliminates the tension between data in some models as shown in [38], but it is not the case with $f(T)$.

Instead of continuing truncating the Union set, now we proceeded to use the latest SNe Ia data set Union2 [3] (processed with SALT2 light-curve fitter [56]) and the combined parameter BAO/CMB. This combined BAO/CMB parameter implemented in [39] is more suitable to add constraints to non-standard models (see Appendix B for details).

The best fit to the Union2 SNe Ia data set only, was achieved with $n = 0.49$ and $\Omega_m = 0.33$ with the reduced $\chi^2_{min}/\nu \simeq 0.98$ (or equivalently, $\Delta\chi^2_{min} = -0.18$ with respect to ΛCDM with $\Omega_m = 0.27$ [4]), where ν is the number of degrees of freedom. All the results with their corresponding 1σ uncertainties and the analysis from the AIC criterion are summarized in Table II.

Working only with the new BAO/CMB parameter we found the value of n for the best fit is remarkably higher than with other data sets ($n = 4.58$), although more efficient in constraining Ω_m (in contrast to working with BAO and CMB parameters separately) having a range of values more consistent with other observations, such as weak lensing and its combination with CMB and SNe Ia (e.g. [57, 58]). In our case we found $\Omega_m = 0.28$. These values ($n = 4.58$, $\Omega_m = 0.28$) perform a better fit than ΛCDM by a $\Delta\chi^2_{min} = -1.46$. Comparing these results with our previous work [22], we also found that including this combined parameter, the value of n for the best fit using BAO/CMB or its combination with the rest of the data sets results always greater than zero. Therefore, the effective dark torsion is of the phantom type [50]. This result is also in opposition with recent constraints when BAO and CMB are used separately through the parameters A and R respectively [26]. Combining the SNe Ia data with BAO/CMB data we found the best fit, which can be seen in Table II.

We added to our analysis a data set of observations of Gamma-Ray Bursts (GRBs). Knowing that there are still debates about if these objects are standard candles (e.g. [59, 60]), we followed the policy assumed in other published works such as [40, 61] to see how our results are modified and to check the consistency of both approaches presented by [61] and [40] in the framework of $f(T)$ theories. Recently, in [62] it has been demonstrated that the data set of [40] is consistent with Union2. One could do the analysis using data sets consisting of SNe Ia and GRBs separately. Otherwise, an analysis can be made compiling Union2 and one GRBs data sets together [61]. These two separate analysis showed identical results (see Appendix A).

Here we used the approach developed in [40] firstly for being a set-independent data set, this means this set is not only applicable with Union2, but with any other SNe Ia data set. Most importantly, we used this data set because evaluating it separately from the SNe Ia is more helpful in our work of finding tension between SNe Ia data and other data sets. Otherwise, in case of finding tension we might have needed to truncate a combination of SNe+GRBs data set, being this last a sum of different data. When incorporating GRBs to the joint statistic we observed that the addition of the mentioned observations slightly reduce the size of the confidence intervals and the joint best fit is displayed in Table II.

In Fig. 2a, we show the confidence intervals of SNe Ia with the combination of SNe+BAO/CMB+GRBs. There, it can be easily seen that with the adopted criterion for the tension between data sets, there is a slight tension between Union2 and the other data sets.

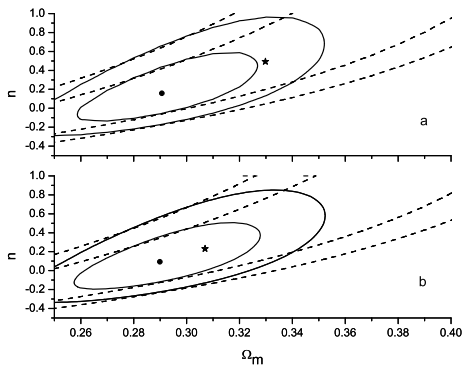

FIG. 2: (a) Confidence intervals at 68.3% and 95.4% in the $\Omega_m - n$ plane for the Union2 observations of SNe Ia only (dashed lines) and Union2 SNe+BAO/CMB+GRBs (solid lines). We also show the best fit values to the observations of Union2 SNe Ia only (star), and to the combination of Union2 SNe+BAO/CMB+GRBs (dot). (b) Idem (a), for the Union2T data set.

In the next section, we will adopt the criterion presented in [37] in order to perform the truncation of Union2 SNe Ia data set with the objective of dissipating the tension between data sets when analyzing these $f(T)$ type of theories.

IV. BUILDING A NEW IMPROVED DATA SET

We followed the simple method used in [36, 37] to find the outliers responsible for the tension. In [36] the distance moduli of the six SNe Ia which are mostly responsible for the tension in Gold06 data set differ by more than 1.8σ from the ΛCDM prediction. In [37] 21 SNe Ia were discarded to build the UnionT set in order to eliminate the tension with CMB and BAO.

Similarly, we firstly fitted our $f(T)$ model to the whole 557 SNe Ia in the Union2 data set and found the best fit parameters (with the corresponding $\mu_0 = 43.15$). Then, we calculated the relative deviation to the best fit prediction, $\mid \mu_{obs} - \mu_{th} \mid /\sigma_{obs}$, for all the 557 data points. We found that as in [37] the cut 1.9σ solved the tension problem. This cut implied to take out 39 SNe Ia from Union2. With the remaining 518 SNe Ia we build the Union2T data set. The outliers are shown in Table I.

TABLE I: The names of the outliers from Union2 data set.

Outliers from Union2
1995ac, 1998dx, 1999bm, 2001v, 2002bf, 2002hd, 2002hu
2002jy, 2003ch, 2003ic, 2006br, 2006cm, 2006cz, 2007ca
10106, 2005ll, 2005lp, 2005fp, 2005gs, 2005gr, 2005hv
2005ig, 2005iu, 2005jj, 1997k, 1998ba, 03D4au, 04D3cp
04D3oe, 03D4cx, 03D1co, d084, e140, f308, g050
g120, m138, 05Str, 2002fx

In Fig. 2b, it is shown the result of using Union2T with the combination of Union2T+BAO/CMB+GRBs. The best fit to Union2T was achieved with the values $n = 0.23$, $\Omega_m = 0.31$ and with $\chi^2_{min}/\nu = 0.67$ ($\Delta\chi^2_{min} = -0.20$), whilst the best fit to the joint analysis of Union2T+BAO/CMB+GRBs was obtained with $n = 0.09$, $\Omega_m = 0.29$ with $\chi^2_{min}/\nu = 0.67$ ($\Delta\chi^2_{min} = -0.97$). From these results we can see that the χ^2_{min} as the χ^2_{min}/ν have been significantly improved in respect to the values obtained in the previous section.

This Union2T set along with the corresponding sets of BAO/CMB and GRBs are more consistent between them, considering the adopted criterion which advantages were mentioned above.

V. ADDING OHD DATA

In this section we wondered about how the results of the previous sections were modified when a data set with Hubble parameter observations $H(z)$ was added to the χ^2 statistic. The details of the used data are displayed in Appendix B.

In Fig. 3a, the confidence intervals are shown at 68.3% and 95.4% for the SNe Ia data only and for the combination of SNe+BAO/CMB+GRBs+OHD. Also, displaying the corresponding best fits. This analysis showed that the best fit was reached with $n = 0.33$ and $\Omega_m = 0.29$ with a $\chi^2_{min}/\nu = 0.96$ ($\Delta\chi^2_{min} = -2.6$). It is observed that the confidence intervals are slightly smaller in size than when OHD data is not added. Surprisingly, we found that the adding of OHD pushes the ΛCDM model out of the 1σ confidence level of the combined data. The inclusion of OHD data, then, favors an equation of state of the phantom type and makes the values that lie at 68.3% to be $n \in [0.12, 0.58]$, $\Omega_m \in [0.27, 0.31]$. A similar result was obtained when combining BAO/CMB, the shift parameter R of CMB and supernovae Ia from SDSS by using the MLCS light-curve fitter (Fig. 1 of [39]).

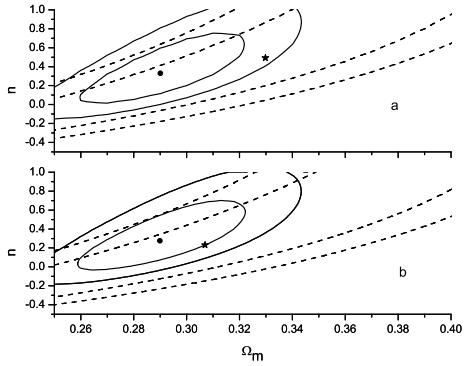

FIG. 3: (a) Confidence intervals at 68.3% and 95.4% in the $\Omega_m - n$ plane for the Union2 observations of SNe Ia only (dashed lines) and Union2 SNe+BAO/CMB+GRBs+OHD (solid lines). We also show the best fit values to the observations of Union2 SNe Ia only (star), and to the combination of Union2 SNe+BAO/CMB+GRBs+OHD (dot). (b) Idem (a), for the Union2T observations.

Again, with the adopted criterion about the existence of tension between data sets we see there is a slight tension between Union2 and Union2 SNe+BAO/CMB+GRBs+OHD. Performing the analogue procedure of the previous section, we found that a 1.9σ cut was suitable to remove the tension between data sets. The result is displayed in Fig. 3b.

The combination Union2T SNe Ia with BAO/CMB, GRBs and OHD allowed the ΛCDM model again to lie inside the 1σ joint probability region.

We summarize in Table II the main results from the analysis performed in this work.

TABLE II: Best fit values and 1σ errors for each parameter marginalizing over the other, for the models considered in this work. (1) SNe, (2) BAO/CMB, (3) SNe + BAO/CMB, (4) SNe + BAO/CMB + GRBs, (5) SNe + BAO/CMB + GRBs + OHD, (6) U2T, (7) U2T + BAO/CMB + GRBs and (8) U2T + BAO/CMB + GRBs + OHD. SNe stands for SNe Ia from Union2 data set, U2T stands for the truncated Union2 data set with a 1.9σ cut and $\Delta AIC = AIC_{f(T)} - AIC_{\Lambda CDM}$.

Data set(s)	n	Ω_m	χ^2_{min}/ν	$\Delta\chi^2_{min}$	ΔAIC
1	$0.49^{+1.13}_{-1.09}$	$0.33^{+0.08}_{-0.19}$	0.98	-0.18	1.82
2	$4.58^{+n/a}_{-4.87}$	$0.28^{+0.02}_{-0.02}$	-	-1.46	0.54
3	$0.15^{+0.28}_{-0.18}$	$0.29^{+0.02}_{-0.02}$	0.97	-0.99	1.00
4	$0.16^{+0.25}_{-0.18}$	$0.29^{+0.02}_{-0.02}$	0.96	-0.93	1.07
5	$0.33^{+0.25}_{-0.21}$	$0.29^{+0.02}_{-0.02}$	0.96	-2.6	-0.60
6	$0.23^{+1.08}_{-0.49}$	$0.31^{+0.08}_{-0.18}$	0.67	-0.20	1.80
7	$0.09^{+0.25}_{-0.18}$	$0.29^{+0.02}_{-0.02}$	0.67	-0.97	1.03
8	$0.28^{+0.24}_{-0.21}$	$0.29^{+0.02}_{-0.02}$	0.67	-1.83	0.17

VI. CONCLUSIONS

We have updated the constraints to an $f(T) = T - \alpha(-T)^{-n}$ theory by using the latest type Ia supernovae data set Union2, the new combined BAO/CMB parameter, a Gamma-Ray Bursts set and Hubble Observational Data.

When the new BAO/CMB parameter is used instead of the frequently used A and R parameters separately the best fit values change with respect to previous works. From Table II we see that all best fit values are for $n > 0$, leading the effective equation of state to be phantom like. Note that in all cases where SNe Ia data were involved, we used the Union2 data set which was processed with SALT2 fitter and this could be an additional factor in the obtained results as showed in [53]. Adding GRB data did not modify the results appreciatively and we also found that two approximations performed by different authors are consistent between them and lead to the same results.

We found that when including information from OHD to put constraints, as in the BAO/CMB case, an equation of state of the phantom type is favored. Remarkably, the simpler ΛCDM model lies outside the 68.3% confidence level region of the combined SNe+BAO/CMB+GRBs+OHD data. The values that lie at 68.3% are in the ranges $n \in [0.12, 0.58]$, $\Omega_m \in [0.27, 0.31]$.

The adopted criterion of tension between data sets in this work and the truncation process performed to Union2 data set allowed us, firstly, that the physics that determines the cosmological evolution through the n parameter does not differ much when only the SNe are considered or when those are combined with other data sets, and secondly, that each data set is consistent amongst the others. In every case, eliminating tension leaded to reduce at least to one half the ratio between values of w_{eff} in $z = 0$ and H in recombination, obtained from the best fits to SNe alone or their combination with other data sets. Additionally, the removal of tension by this criterion resulted in, when combining Union2T data set with BAO/CMB+GRB+OHD, the ΛCDM model to lie inside the 1σ joint probability region of the data set with all observations. From Table II, the values for $\Delta\chi^2_{min}$ always favored the $f(T)$ models, whilst when performing an analysis with the AIC criterion we found that all the evaluated cases of $f(T)$ have the same support from the data with respect to the ΛCDM model since $0 < |\Delta AIC| < 2$.

Acknowledgments

G.R.B. is supported by CONICET. I would like to thank Eric Linder for kind dialogues, to Ariel Goobar, Hao Wei and Lixin Xu for helpful discussions. Also, I thank Diego Travieso for his numerical collaboration and interesting discussions and Rafael Ferraro for his support.

Appendix A: Analysis from Hymnium Gamma-Ray Bursts data set

Here we show the result of adding to the performed analysis with the Union2 SNe Ia data set, the set Hymnium of 59 GRBs according to [61].

With the objective of comparing the obtained results when adding GRBs to SNe Ia data and BAO/CMB using the 5 values set of [40] and when adding the data sets in the way performed in [61], we observed the differences in the 68.3% and 95.4% confidence intervals of both methods. The result using the 59 GRBs set of [61] is displayed in Fig. 4. The values in the joint best fit are for $n = 0.15^{+0.26}_{-0.18}$ and $\Omega_m = 0.29^{+0.02}_{-0.02}$. As can be seen, the result is very similar to the one obtained in section III (Fig. 2a).

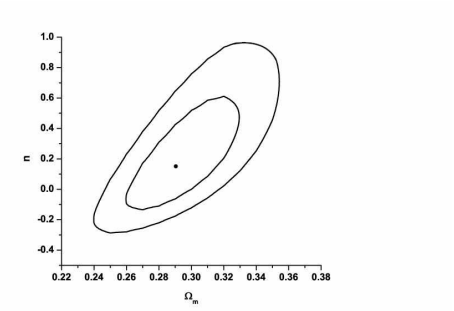

FIG. 4: Confidence intervals at 68.3% and 95.4% in the $\Omega_m - n$ plane coming from combining SNe+GRBs+BAO/CMB data, where the 59 GRBs from the Hymnium data set were added to Union2 according to [61].

Appendix B: Cosmological constraints methods

1. Type Ia Supernovae constraints

The data points of the 557 Union2 SNe Ia compiled in [3] are given in terms of the distance modulus $\mu_{obs}(z_i)$ and the corresponding uncertainty for each observed value $\sigma(z_i)$. On the other hand, the theoretical distance modulus is defined as

$$\mu_{th}(z_i) = 5log_{10}D_L(z_i) + \mu_0 \tag{B1}$$

where $\mu_0 \equiv 42.38 - 5log_{10}h$ and h is the Hubble constant H_0 in units of 100 km/s/Mpc, whereas the Hubble-free luminosity distance for the flat case is

$$D_L(z) = (1+z)\int_0^z \frac{dz'}{E(z',\mathbf{p})} \tag{B2}$$

in which $E \equiv H/H_0$, and $\mathbf{p}$ denotes the model parameters (here, n and Ω_m). The parameter μ_0 is a nuisance parameter but it is independent of the data points. Following [63], the minimization with respect to μ_0 can be made by expanding the χ^2_{SNe} with respect to μ_0 as

$$\chi^2_{SNe}(\mathbf{p}) = \tilde{A} - 2\mu_0\tilde{B} + \mu_0^2\tilde{C} \tag{B3}$$

where,

$$\begin{aligned}
\tilde{A}(\mathbf{p}) &= \sum_{i=1}^{N=557} \frac{[\mu_{obs}(z_i) - \mu_{th}(z_i;\mu_0=0,\mathbf{p})]^2}{\sigma^2(z_i)} \\
\tilde{B}(\mathbf{p}) &= \sum_{i=1}^{N=557} \frac{[\mu_{obs}(z_i) - \mu_{th}(z_i;\mu_0=0,\mathbf{p})]}{\sigma^2(z_i)} \\
\tilde{C} &= \sum_{i=1}^{N=557} \frac{1}{\sigma^2(z_i)}
\end{aligned}$$

Equation (B3) has a minimum for $\mu_0 = \tilde{B}/\tilde{C}$ at

$$\tilde{\chi}^2_{SNe}(\mathbf{p}) = \tilde{A}(\mathbf{p}) - \frac{\tilde{B}(\mathbf{p})^2}{\tilde{C}} \tag{B4}$$

Since $\chi^2_{SNe,min} = \tilde{\chi}^2_{SNe,min}$ obviously, we can instead minimize $\tilde{\chi}^2_{SNe}$ which is independent of μ_0.

2. Combined BAO/CMB parameter constraints

In the $f(T)$ theories considered here (10), for later times the term $-\alpha/(-T)^n$ is dominant, while in early times when $H \to \infty$ General Relativity is recovered. Also, since this model presents matter domination at the decoupling time as the standard model, we can use the BAO and CMB information as showed in [22].

When analyzing CMB and BAO observations there are two parameters commonly employed, R [64] and A [54]. However, a more model-independent constraint can be achieved by multiplying the BAO measurement of $r_s(z_d)/D_V(z)$ with the position of the first CMB power spectrum peak [55] $\ell_A = \pi d_A(z_*)/r_s(z_*)$, thus cancelling some of the dependence on the sound horizon scale [39]. Here, $d_A(z_*)$ is the comoving angular-diameter distance to recombination, r_s is the comoving sound horizon at photon decoupling, $z_d \approx 1020$ is the redshift of the drag epoch at which the acoustic oscillations are frozen in, and D_V is defined as (assumed a ΛCDM model) [54],

$$D_V(z) = \left[\frac{z}{H(z)}\left(\int_0^z \frac{dz'}{H(z')}\right)^2\right]^{1/3} \tag{B5}$$

We further assume $z_* = 1090$ from [55] (variations within the uncertainties about this value do not give significant differences in the results).

In [65] was measured $r_s(z_d)/D_V(z)$ at two redshifts, $z = 0.2$ and $z = 0.35$, finding $r_s(z_d)/D_V(0.2) = 0.1905 \pm$

0.0061 and $r_s(z_d)/D_V(0.35) = 0.1097 \pm 0.0036$. Combining this with ℓ_A gives the combined BAO/CMB constraints [39]:

$$\begin{aligned} \frac{d_A(z_*)}{D_V(0.2)}\,\frac{r_s(z_d)}{r_s(z_*)} &= 18.32 \pm 0.59 \\ \frac{d_A(z_*)}{D_V(0.35)}\,\frac{r_s(z_d)}{r_s(z_*)} &= 10.55 \pm 0.35 \end{aligned} \tag{B6}$$

Before matching to cosmological models we also need to implement the correction for the difference between the sound horizon at the end of the drag epoch and the sound horizon at last scattering. The first is relevant for the BAO, the second for the CMB, and $r_s(z_d)/r_s(z_*) = 1.044 \pm 0.019$ (using values from [55]). Inserting this into (B6) and taking into account the correlation between these measurements using the correlation coefficient of 0.337 calculated by [65], gives the final constraints we use for the cosmology analysis [39]:

$$\begin{aligned} A_1 = \frac{d_A(z_*)}{D_V(0.2)} &= 17.55 \pm 0.65 \\ A_2 = \frac{d_A(z_*)}{D_V(0.35)} &= 10.10 \pm 0.38 \end{aligned} \tag{B7}$$

Using this BAO/CMB parameter cancels out some of the dependence on the sound horizon size at last scattering. This thereby removes the dependence on much of the complex pre-recombination physics that is needed to determine that horizon scale [39]. In all the cases, we have considered a radiation component $\Omega_r = 5x10^{-5}$.

So, for our analysis we add to the χ^2 statistic:

$$\chi^2_{BAO/CMB}(\mathbf{p}) = \sum_{i=1}^{N=2} \frac{[A_{obs}(z_i) - A_{th}(z_i;\mathbf{p})]^2}{\sigma_A^2(z_i)} \tag{B8}$$

where $\mathbf{p} = (n, \Omega_m)$ are the free parameters, A_{obs} is the observed value (A_1 and A_2), A_{th} is the predicted value by the model and σ_A is the 1σ error of each measurement.

3. Gamma-Ray Bursts constraints

Following [66] and [40], we consider the well-known Amati's $E_{p,i} - E_{iso}$ correlation [67–70] in GRBs, where $E_{p,i} = E_{p,obs}(1+z)$ is the cosmological rest-frame spectral peak energy, and E_{iso} is the isotropic energy.

In [71], it was defined a set of model-independent distance measurements $\{\bar{r}_p(z_i)\}$:

$$\bar{r}_p(z_i) \equiv \frac{r_p(z)}{r_p(z_0)} \tag{B9}$$

with,

$$r_p(z) \equiv \frac{(1+z)^{1/2}}{z}\,\frac{H_0}{c}\,r(z) \tag{B10}$$

where $r(z) = d_L(z)/(1+z)$ is the comoving distance at redshift z, and $z_0 = 0.0331$ is the lowest GRBs redshift.

Following the method proposed by [71], in [40] were obtained 5 model-independent distances data points and their covariance matrix by using 109 GRBs via Amati's correlation. The resulted model-independent distances $\bar{r}_p^{data}(z_i)$ and their uncertainties, the correlation matrix and the covariance matrix are these ones from [40].

So, a given cosmological model with $\{\mathbf{p}\}$ free parameters can be constrained by GRBs via

$$\chi^2_{GRB}(\mathbf{p}) = [\Delta\bar{r}_p(z_i)]^T \cdot (\mathbf{C}^{-1}_{GRB}) \cdot [\Delta\bar{r}_p(z_i)] \tag{B11}$$

$$\Delta\bar{r}_p(z_i) = \bar{r}_p^{data}(z_i) - \bar{r}_p(z_i) \tag{B12}$$

where $\bar{r}_p(z_i)$ is defined by (B9) and $\mathbf{C}^{-1}_{GRB}$ is the inverse of the covariance matrix. In this way, the constraints for a large amount of observational GRBs data is projected into the relative few quantities $\bar{r}_p^{data}(z_i)$.

4. Observational Hubble Data (OHD) constraints

The Observational Hubble Data are based on differential ages of the galaxies [72]. In [73] it was obtained an independent estimate for the Hubble parameter using the method developed in [72], and the authors used it to constrain the equation of state of dark energy. The Hubble parameter depending on the differential ages as a function of redshift can be written as,

$$H(z) = -\frac{1}{1+z}\,\frac{dz}{dt} \tag{B13}$$

So, once dz/dt is known, $H(z)$ is obtained directly [74]. By using the differential ages of passively-evolving galaxies, in [74] was obtained $H(z)$ in the range of $0.1 \lesssim z \lesssim 1.8$ and in [43] new data at $0.35 < z < 1$ were studied. Here, H_0 from [42] and eleven observational Hubble data from [43] are used.

In addition, in [41] the authors took the BAO scale as a standard ruler in the radial direction, called "Peak Method", obtaining three more additional data (in km/s/Mpc): $H(z = 0.24) = 79.69 \pm 2.32$, $H(z = 0.34) = 83.8 \pm 2.96$ and $H(z = 0.43) = 86.45 \pm 3.27$, which are model- and scale-independent. We just consider the statistical errors.

The best fit values of the cosmological model parameters from observational Hubble data are then determined by minimizing,

$$\chi^2_{OHD}(\mathbf{p}) = \sum_{i=1}^{N=15} \frac{[H_{obs}(z_i) - H_{th}(z_i;\mathbf{p})]^2}{\sigma^2(z_i)} \tag{B14}$$

where as before, in this work $\mathbf{p} = (n, \Omega_m)$, H_{th} is the predicted value for the Hubble parameter, H_{obs} is the observed value, $\sigma(z_i)$ is the standard deviation of each measurement, and the summation is over the full 15 values at redshift z_i mentioned above.

[1] Perlmutter S. et al., Bull. Am. Astron. Soc. **29**, (1997) 1351; Astrophys. J. **517**, (1999) 565; Riess A. G. et al., Astron. J. **116**, (1998) 1009; Astron. J. **607** (2004) 665.
[2] Kowalski M. et al., Astrophys. J. **686**, (2008) 749.
[3] Amanullah R. et al., Astrophys. J. **716**, (2010) 712.
[4] Komatsu E. et al., arXiv:1001.4538.
[5] Sahni V. and Starobinsky A. A., Int. J. Mod. Phys. **D9**, (2000) 373.
[6] Padmanabhan T., Phys. Rep. **380**, (2003) 235.
[7] Frieman J., Turner M. S. and Huterer D., Annu. Rev. Astron. Astrophys. **46**, (2008) 385.
[8] Buchdahl H. A., Mon. Not. R. Astron. Soc. **150**, (1970) 1.
[9] Starobinsky A. A., Phys. Lett. **B91**, (1980) 99.
[10] Kerner R., Gen. Relat. Gravit. **14**, (1982) 453.
[11] Barrow J. D. and Ottewill A. C., J. Phys. A: Math. Gen. **16**, (1983) 2757.
[12] Barrow J. D. and Cotsakis S., Phys. Lett. **B214**, (1988) 515.
[13] Carroll S. M. et al., Phys. Rev. **D70**, (2004) 043528.
[14] Starobinsky A. A., JETP Lett. **86**, (2007) 157.
[15] Hu W. and Sawicki I., Phys. Rev. **D76**, (2007) 064004.
[16] Nojiri S. and Odintsov S. D., arXiv:0807.0685.
[17] Nojiri S and Odintsov S. D., Int. J. Geom. Meth. Mod. Phys. **4**, (2007) 115.
[18] Capozziello S. and Francaviglia M., Gen. Relat. Gravit. **40**, (2008) 357.
[19] Sotiriou T. and Faraoni V., Rev. Mod. Phys. **82**, (2010) 451.
[20] Ferraro R. and Fiorini F., Phys. Rev. **D75**, (2007) 084031.
[21] Ferraro R. and Fiorini F., Phys.Rev. **D78**, (2008) 124019.
[22] Bengochea G. R. and Ferraro R., Phys. Rev. **D79**, (2009) 124019.
[23] Einstein A., Sitzungsber. Preuss. Akad. Wiss. Phys. Math. KI.,(1928) 217; ibid., (1930) 401; Einstein A., Math. Annal. **102**, (1930) 685.
[24] Hayashi K. and Shirafuji T., Phys. Rev. **D19**, (1979) 3524, Addendum-ibid. **D24**, (1982) 3312.
[25] Linder E. V., Phys. Rev. **D81**, (2010) 127301.
[26] Wu P. and Yu H., Phys. Lett. **B693**, (2010) 415.
[27] Wu P. and Yu H., Phys. Lett. **B692**, (2010) 176.
[28] Wu P. and Yu H., arXiv:1008.3669.
[29] Myrzakulov R., arXiv:1006.1120; arXiv:1008.4486.
[30] Yerzhanov K. K. et al., arXiv:1006.3879.
[31] Yang R. J., arXiv:1007.3571; arXiv:1010.1376.
[32] Karami K. and Abdolmaleki A., arXiv:1009.2459; arXiv:1009.3587.
[33] Dent J. B. et al., arXiv:1008.1250; arXiv:1010.2215.
[34] Li B. et al., arXiv:1010.1041.
[35] Bamba K. et al., arXiv:1008.4036; Bamba K. et al., arXiv:1011.0508.
[36] Nesseris S. and Perivolaropoulos L., JCAP **0702**, (2007) 025.
[37] Wei H., Phys. Lett. **B687**, (2010) 286.
[38] Li M. et al., arXiv:0910.0717.
[39] Sollerman J. et al., Astrophys. J. **703**, (2009) 1374.
[40] Xu L. and Wang Y., Phys. Rev. **D82**, (2010) 043503; Xu L., arXiv:1005.5055.
[41] Gaztanaga E. et al., MNRAS **399**, (2009) 1663.
[42] Riess A. G. et al., Astrophys. J. **699**, (2009) 539.
[43] Stern D. et al., JCAP **02**, (2010) 008.
[44] Weitzenböck R., *Invarianten Theorie*, (Nordhoff, Groningen, 1923).
[45] Maluf J. W., J. Math. Phys. **35**, (1994) 335.
[46] Arcos H. and Pereira J., Int. J. Mod. Phys. D**13**, (2004) 2193.
[47] Akaike H., IEEE Trans. Auto. Control, **19**, (1974) 716.
[48] Liddle A. R., MNRAS **351**, (2004) L49.
[49] Biesiada M., JCAP **702**, (2007) 003.
[50] Caldwell R. R., Phys. Lett. **B545**, (2002) 23.
[51] Kessler R. et al., Astrophys. J. Suppl. Ser. **185**, (2009) 32.
[52] Phillips M. M. et al., Astrophys. J. **413**, (1993) L105; Riess A. G. et al., Astrophys. J. **438**, (1995) L17; Jha S. et al., Astrophys. J. **659**, (2007) 122.
[53] Bengochea G. R., Phys. Lett. **B** (2010), doi:10.1016/j.physletb.2010.12.014, arXiv:1010.4014.
[54] Eisenstein D. et al., Astrophys. J. **633**, (2005) 560.
[55] Komatsu E. et al., Astrophys. J. Suppl. **180**, (2009) 330.
[56] Guy J. et al., Astron. and Astrophys. **466**, (2007) 11.
[57] Jarvis M. et al., Astrophys. J. **644**, (2006) 71.
[58] Schrabback T. et al., Astron. and Astrophys. **516**, (2010) A63.
[59] Ghirlanda E. et al., New J. Phys. **8**, (2006) 123.
[60] Basilakos S. and Perivolaropoulos L., MNRAS **391**, (2008) 411.
[61] Wei H., JCAP **08**, (2010) 020.
[62] Xu L. and Wang Y., arXiv:1007.4734.
[63] Nesseris S. and Perivolaropoulos L., Phys. Rev. **D72**, (2005) 123519; Perivolaropoulos L., Phys. Rev. **D71**, (2005) 063503.
[64] Bond J. R. et al., MNRAS **291**, (1997) L33.
[65] Percival W. J. et al., MNRAS **401**, (2010) 2148.
[66] Schaefer B. E., Astrophys. J. **660**, (2007) 16.
[67] Amati L. et al., Astron. and Astrophys. **390**, (2002) 81.
[68] Amati L. et al., MNRAS **391**, (2008) 577.
[69] Amati L., MNRAS **372**, (2006) 233.
[70] Amati L. et al., Astron. and Astrophys. **508**, (2009) 173.
[71] Wang Y., Phys. Rev. **D78**, (2008) 123532.
[72] Jimenez R. and Loeb A., Astrophys. J. **573**, (2002) 37.
[73] Jimenez R. et al., Astrophys. J. **593**, (2003) 622.
[74] Simon J. et al., Phys. Rev. **D71**, (2005) 123001.